Proceedings of the 6th International Symposium
on
Advanced Nuclear Energy Research
—INNOVATIVE LASER TECHNOLOGIES IN NUCLEAR ENERGY—

Simulations of Longitudinally Pumped Dye Laser Amplifier

Kiwamu Takehisa and Satoshi Takemori

Hitachi Research Laboratory, Hitachi Ltd.,
7-1-1, Ohmika-cho, Hitachi-shi, 319-12 Japan
Tel. 0294-36-8413, Fax. 0294-36-8398

Simulations of a copper laser pumped dye laser amplifier and new designs of the longitudinally pumped dye laser amplifier are presented. The simulations take the consideration of the amplified spontaneous emission (ASE). The new designs utilize a center-hole reflector instead of a dichroic mirror. The simulation results indicate that the poor spatial overlap between the pump beam and the dye beam in the transverse pumping not only reduces the laser output power, but also generates ASE strongly. The results also indicate that the longitudinal pumping is as efficient as the transverse pumping.

Keywords: Dye laser, Transverse pumping, Longitudinal pumping, ASE

1. Introduction

Copper laser pumped dye lasers have been developed to more than 1 kW output power especially for use in atomic vapor laser isotope separation (AVLIS).[1, 2] In such high-power dye lasers, their amplifiers are transversely pumped. However, longitudinal pumping is more widely used for diode-pumped YAG lasers, because of a good spatial overlap achievable between the laser beam and the pump beam.

Typical configurations of the transverse pumping and the longitudinal pumping for a copper laser pumped dye laser amplifier are illustrated in Fig.1. One of the most serious problems in each pumpings are as follows. In the transverse pumping, the pumped area has a rectangular cross section, more elaborate optical techniques are required to achieve good spatial overlap between the pump beam and the dye beam. For example, beam reforming optics are used for the pump beams to be rectangular,

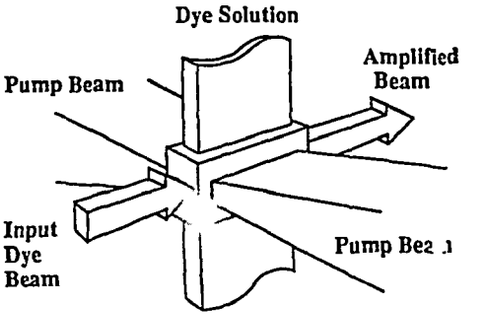

(a) Transverse Pumping

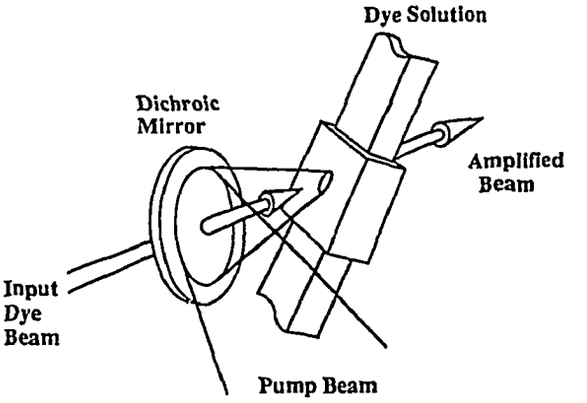

(b) Longitudinal Pumping

Fig.1 Configurations of the transverse Pumping and the longitudinal Pumping

and/or relay telescope optics are used for the dye beam if its cross section is rectangular. The poor spatial overlap not only reduces the utilization efficiency of the pump power, but also generates amplified spontaneous emission (ASE) strongly.[3]
Another problem with the transverse pumping is that the intensity profile of the amplified output is likely to be inhomogeneous, especially as the dye concentration increases.

While in the longitudinal pumping, dichroic mirrors are necessary, which brings two problems in the case of the copper laser pumped high power dye lasers. First, dichroic mirrors give a 5-10% power loss in the pump beam or/and the dye beam because the wavelength difference between the copper laser and the dye laser is small compared with a case of diode-pumped YAG lasers. Secondary, dichroic mirrors are more easily damaged by the high intensity dye beam than AR coated optics.

In this paper, we show the simulation results of the transverse pumping with a consideration of ASE, and also propose new designs for the longitudinal pumping without dichroic mirrors.

2. Simulations for transverse pumping

ASE from the dye lasers have been analyzed mostly by a one-dimensional model. However it is almost impossible for those analyses to evaluate the spatial overlap between the pump beam and the dye beam. Therefore a three-dimensional model is used in the simulations.[3] Since ASE has quite a large beam divergence, the propagating directions of the angularly divided ASE are taken into considerations (see Fig.2). ASE of its direction close to the Z axis is considered, and it is divided into two counter-propagating ASE: forward travelling ASE (F.ASE) and backward travelling ASE (B.ASE). The simulation are based on the rate equations for the energy levels shown in Fig.3.

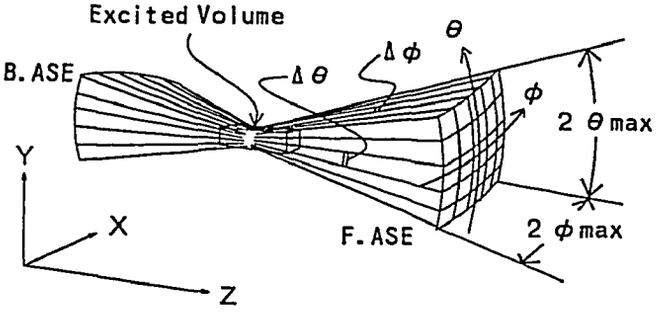

Fig.2 Illustration of forward and backward ASE divided angularly.

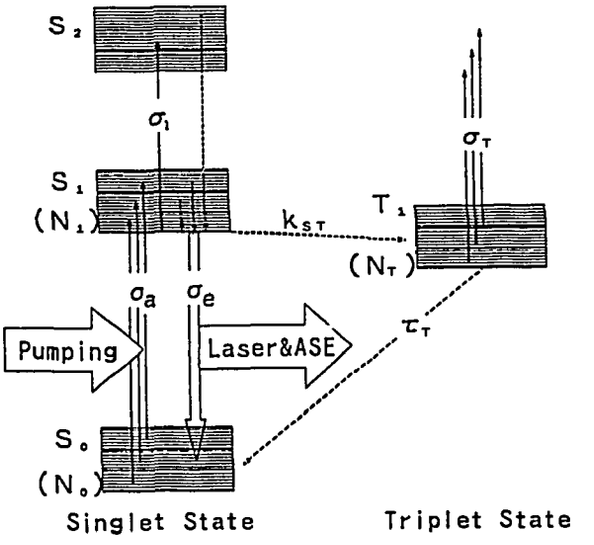

Fig.3 Energy levels of the dye molecule used in the simulations.

The equations are expressed as the followings with parameters listed in Table I.

$$\frac{\partial N_1(t,x,y,z)}{\partial t} = c\,(\sigma a(\lambda p)\,N_0(t,x,y,z) - \sigma e(\lambda p)\,N_1(t,x,y,z))\,N_p(t,x,y,z) + c\,(\sigma a(\lambda_L)\,N_0(t,x,y,z) - \sigma e(\lambda_L)\,N_1(t,x,y,z))\,N_L(t,x,y,z) + c\,(\sigma a(\lambda_{ASE})\,N_0(t,x,y,z) - \sigma e(\lambda_{ASE})\,N_1(t,x,y,z))\sum_{\phi}\sum_{\theta} N_{ASE}(t,x,y,z,\phi,\theta) - (k_{ST} + t_S^{-1})\,N_1(t,x,y,z) \quad (1)$$

$$\frac{\partial N_T(t,x,y,z)}{\partial t} = k_{ST}\,N_1(t,x,y,z) - t_T^{-1}\,N_T(t,x,y,z) \quad (2)$$

$$\frac{\partial N_L(t,x,y,z)}{\partial z} + \frac{1}{c}\frac{\partial N_L(t,x,y,z)}{\partial t} = (\sigma e(\lambda_L)\,N_1(t,x,y,z) - \sigma a(\lambda_L)\,N_0(t,x,y,z) - \sigma_S(\lambda_L)\,N_1(t,x,y,z) - \sigma_T(\lambda_L)\,N_T(t,x,y,z))\,N_L(t,x,y,z) \quad (3)$$

$$\frac{\partial N_{ASE}(t,x,y,z,\phi,\theta)}{\partial z} + \frac{1}{c}\frac{\partial N_{ASE}(t,x,y,z,\phi,\theta)}{\partial t} = (\sigma e(\lambda_{ASE})\,N_1(t,x,y,z) - \sigma a(\lambda_{ASE})\,N_0(t,x,y,z) - \sigma_S(\lambda_{ASE})\,N_1(t,x,y,z) - \sigma_T(\lambda_{ASE})\,N_T(t,x,y,z))\,N_{ASE}(t,x,y,z,\phi,\theta) \quad (4)$$

$$N = N_1(t,x,y,z) + N_0(t,x,y,z) + N_T(t,x,y,z). \quad (5)$$

TABLE I Explanations of the parameters used in the simulations.

Parameter	Quantity	Value	Unit
N_0	Population Density in the S_0 State		m^{-3}
N_1	Population Density in the S_1 State		m^{-3}
N_T	Population Density in the S_T State		m^{-3}
Np	Population Density of the Pump Beam		m^{-3}
N_L	Population Density of the Laser Beam		m^{-3}
λp	Wavelength of the Pump Beam	510.6×10^{-9}	m
λ_L	Wavelength of the Laser Beam	580×10^{-9}	m
λ_{ASE}	Center wavelength of ASE	580×10^{-9}	m
$\sigma a(\lambda p)$	Absorption Cross Section for S_0 - S_1 at 510.6 nm	1.3×10^{-20}	m^2
$\sigma e(\lambda p)$	Emission Cross Section for S_0 - S_1 at at 510.6 nm	0.0	m^2
$\sigma e(\lambda_L)$, $\sigma e(\lambda_{ASE})$	Emission Cross Section for S_0 - S_1 at 580 nm	1.6×10^{-20}	m^2
$\sigma a(\lambda_L)$, $\sigma a(\lambda_{ASE})$	Absorption Cross Section for S_0 - S_1 at 580 nm	3.0×10^{-22}	m^2
$\sigma_S(\lambda p)$	Absorption Cross Section for S_1 - S_2 at 510.6 nm	4.0×10^{-21}	m^2
$\sigma_S(\lambda_L)$, $\sigma_S(\lambda_{ASE})$	Absorption Cross Section for S_1 - S_2 at 580 nm	2.0×10^{-21}	m^2
$\sigma_T(\lambda_L)$, $\sigma_T(\lambda_{ASE})$	Absorption Cross Section for T_1 - T_2 at 580 nm	6.5×10^{-21}	m^2
$\sigma_T(\lambda p)$	Absorption Cross Section for T_1 - T_2 at 510.6 nm	0.0	m^2
k_{ST}	S_1 - T_1 Intersystem Crossing Rate	3.0×10^{6}	s^{-1}
τ_S	S_1 State Lifetime	3.5×10^{-9}	s
τ_T	T_1 - S_0 Relaxation Time	2.7×10^{-7}	s
c	Light Speed in the Medium	2.2×10^{8}	ms^{-1}

ASE photon transfer equations are more complicated than the laser photon because the ASE propagates not only toward the ±Z directions, it also shifts to the X and Y directions. Therefore in the simulations, ASE in one meshed area is programmed to transfer dividedly into the adjacent 8 meshed areas at every interval of Δt (=Δz/c) (see Fig.4). The rate of the each division is proportional to the overlapped mesh volume.

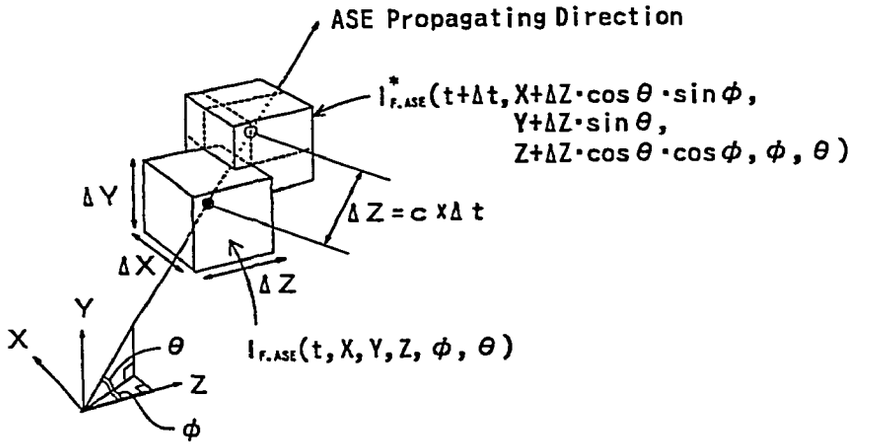

Fig.4 ASE propagation in the meshed area.

The calculation conditions are shown in Table II. In order to evaluate the temporal overlap between the pump beam and the dye beam, laser output power and F.ASE power as a function of the input dye beam delay time is calculated. The results shown in Fig.5 indicate that the temporal mismatching generates ASE.

TABLE II. Calculation conditions.

Quantity	Value
Pulse repetition rate	5 kHz
Laser pulse duration time	100 ns
Laser pulse shape	sine wave
Input beam intensity	homogeneous
Active volume	
Width	2 mm
Height	2 mm
Length	20 mm
Dye concentration	0.2 mmol/l

To evaluate the effect of the spatial overlap, laser output power and the F.ASE power as a function of the input dye beam width is calculated. From the results shown in Fig.6, ASE is decreased as the width increases, and is negligibly small when the width is 2.0 mm, in which the input dye beam covers all the pumped area. Therefore ASE is considered to generate from the part of the pumped area where there is no input signal.

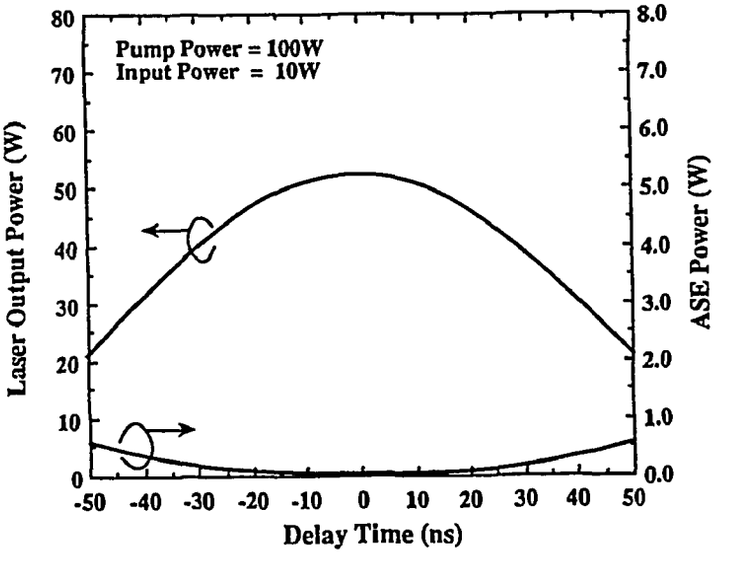

Fig.5 Laser output power and F.ASE power as a function of the delay time.

Concerning the intensity profile, the amplified output beam becomes inhomogeneous if the input beam is homogeneous. The inhomogeneity can be reduced by reducing the dye concentration. However as the dye concentration decreases, the pump beams are less absorbed in the dye solution, which results in decreasing the extraction efficiency. In Fig.7 the extraction efficiency is calculated as a function of the dye concentration. The intensity inhomogeneity, defined as the minimum intensity divided by the maximum intensity, is also calculated. The results suggest that the maximum extraction efficiency is obtained with the concentration of about 0.2 mmol/l and the inhomogeneity is about 0.5.

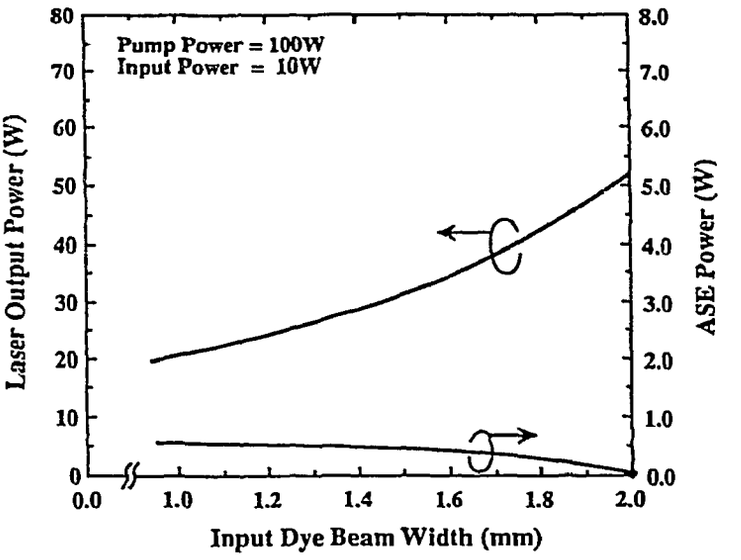

Fig.6 Laser output power and F.ASE power as a function of the input dye beam width.

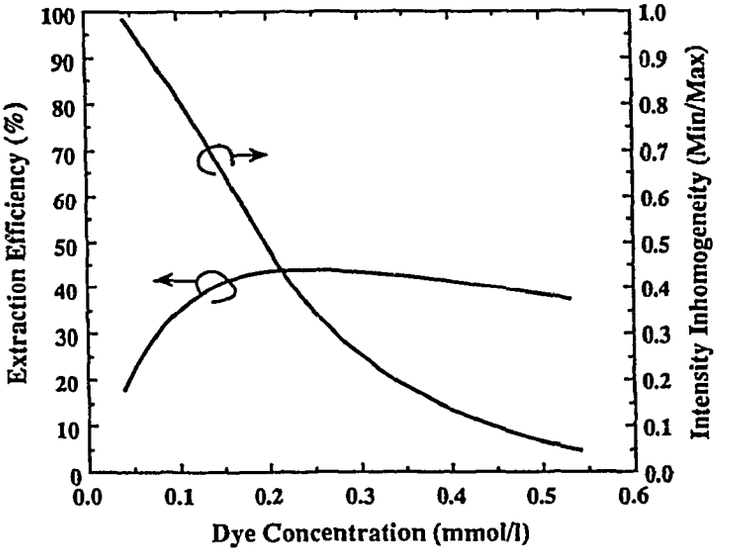

Fig.7 Extraction efficiency and intensity inhomogeneity as a function of the dye concentration.

3. New designs of longitudinal pumping [4]

Our proposed configuration for the longitudinal pumping is illustrated in Fig.8. Instead of a dichroic mirror, a center-hole mirror (CHM) is used to introduce the pump beam colinearly with the dye beam. This technique has been demonstrated for pumping a Ti:sapphire laser oscillator.[5] Comparison with a dichroic mirror, the CHM can have less power loss of about 1 %, because the beam diameter of the dye laser is much smaller than that of the copper laser. In addition to this, there is no possibility of incurring damage by the high-intensity dye beam.

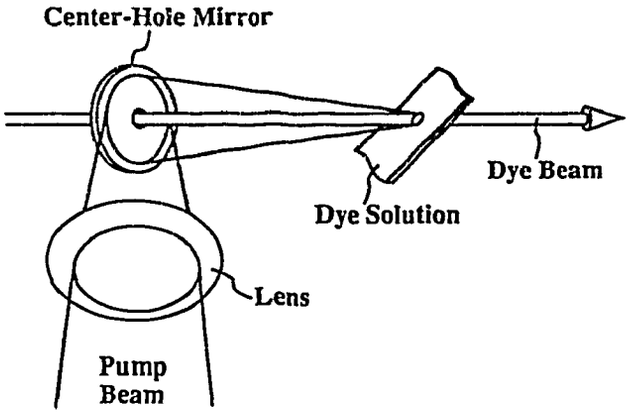

Fig. 8 Proposed new design for the longitudinal pumping.

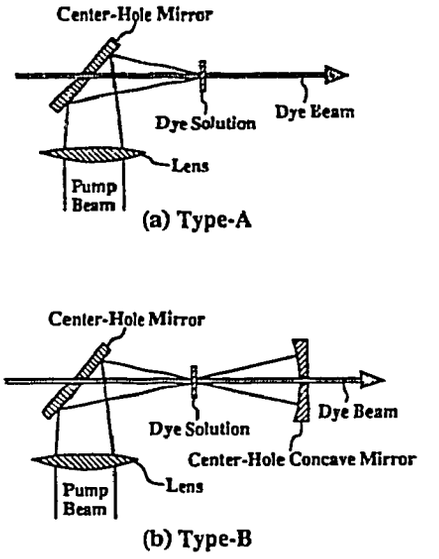

Fig. 9 Three variations of the new design.

Three different types of the new configuration (Type-A, B, and C) are simulated (see Fig.9). Type-A is the same as shown in Fig.8. Type-B utilizes a center-hole concave mirror which reflects the transmitted pump beam back into the dye solution. Type-C utilizes two counter propagating pump beams.

In the simulation, the dye beam and the pump beam are assumed to be overlapped completely, and they have a homogeneous intensity profile. Therefore, one-dimensional model is used, in which a circular beam is assumed with the diameter of 2 mm. For the Type-B and the Type-C, the pump photon density $N_P(t,z)$ of the counter-propagating pump beams is considered, and is expressed as:

$$N_P(t,z) = N_P^+(t,z) + N_P^-(t,z) \tag{6}$$

where $N_P^+(t,z)$ represents the density of the forward travelling pump photon, and $N_P^-(t,z)$ represents that of the backward travelling pump photon. The rate equations are

$$\frac{\partial N_P^+(t,z)}{\partial z} + \frac{1}{c}\frac{\partial N_P^+(t,z)}{\partial t} = \left(\sigma e(\lambda_P)\, N_1(t,z) - \sigma a(\lambda_P)\, N_0(t,z) - \sigma_S(\lambda_P)\, N_1(t,z) - \sigma_T(\lambda_P)\, N_T(t,z) \right) N_P^+(t,z) \tag{7}$$

$$\frac{\partial N_P^-(t,z)}{\partial z} + \frac{1}{c}\frac{\partial N_P^-(t,z)}{\partial t} = \left(\sigma e(\lambda_P)\, N_1(t,z) - \sigma a(\lambda_P)\, N_0(t,z) - \sigma_S(\lambda_P)\, N_1(t,z) - \sigma_T(\lambda_P)\, N_T(t,z) \right) N_P^-(t,z). \tag{8}$$

In the simulation, the absorption length of the pump beam is used as a parameter instead of the dye concentration. Since the ratio of the active length L to the absorption length La dominates the rate of the absorbed pump power, laser output power as a function of the active length is calculated for the Type-A with a parameter of L/La. The results are shown in Fig.10. It is clear that if L/La is kept constant, almost the same output power can be obtained. This makes it possible to reduce the dye flow rate by decreasing the active length. Moreover, once L/La is kept at its optimum, the same dye concentration can be used at every stage of the amplifier chain.

To obtain the optimum of L/La for each type, laser output power as a function of L/La is calculated. From the results shown in Fig.11, it is cleared that the optimum of L/La depends on the pumping schemes.

Laser output power as a function of the pump power is calculated with L/La = 5.5 for Type-A, L/La = 4 for Type-B, and L/La = 6 for Type-C. Results are shown in Fig.12. These L/La values are the optimum for each pumping schemes obtained from Fig.11. For comparison, laser output power for the transverse pumping is also calculated. The results indicate that every type of the longitudinal pumping are as efficient as the transverse pumping, and that Type-C gives a little higher output power in the calculated range.

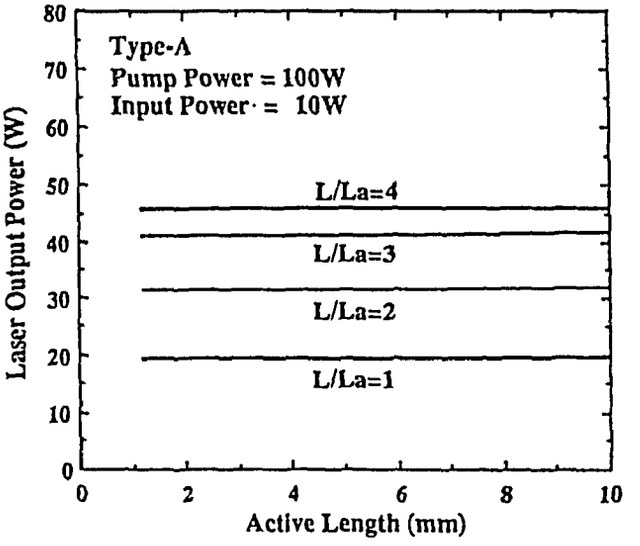

Fig.10 Laser output power as a function of the active length as a parameter of L/La.

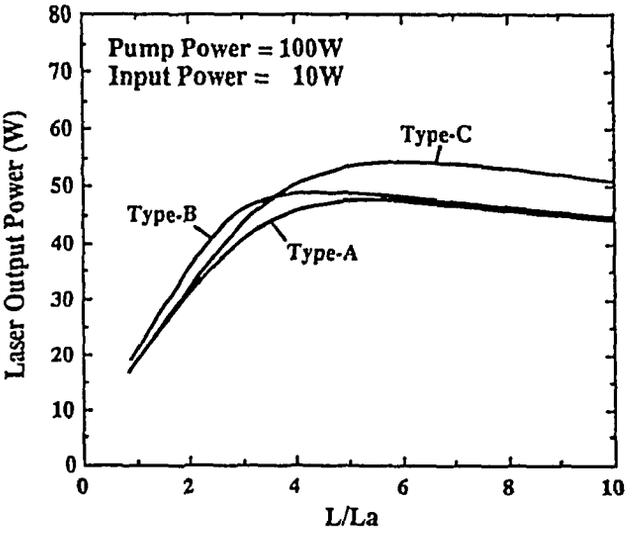

Fig. 11 Laser output power as a function of L/La.

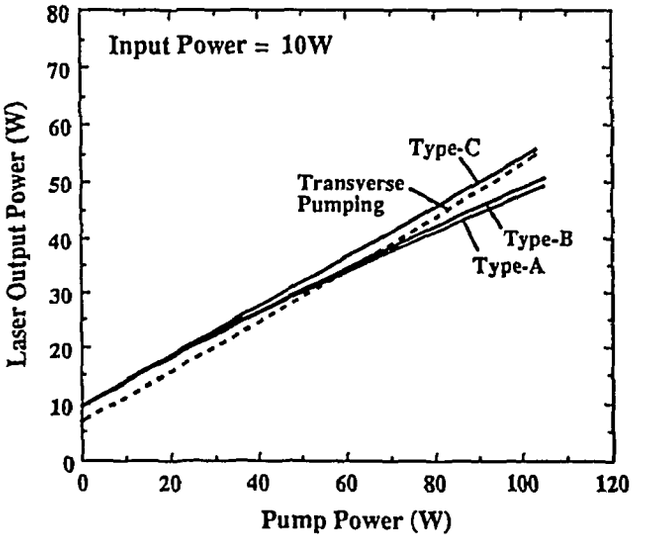

Fig.12 Laser output power as a function of the pump power.

4. Conclusions

Simulations of a copper laser pumped dye laser amplifier were presented. The simulation results of the transverse pumping considering ASE have cleared that the poor spatial overlap between the pump beam and the dye beam not only reduces the laser output power, but also generate the ASE strongly. Proposed new designs of the longitudinal pumping can avoid the problems caused by a dichroic mirror. Simulation results of the new designs have suggested that the longitudinal pumping is as efficient as the transverse pumping.

5. References

1) I. L. Bass, R. E. Bonanno, R. P. Hackel, and P. R. Hammond, "High-average-power dye laser at Lawrence Livermore National Laboratory," Appl. Optics, vol.31, pp.6993-7006 (1992).
2) R. P. Hackel, B. E. Warner, "The copper-pumped dye laser system at Lawrence Livermore National Laboratory," SPIE Vol. 1859 Laser Isotope Separation, pp.120-129 (1993).
3) K. Takehisa, H. Nishimura, and A. Miki, "Three-dimensional simulation of dye laser amplifiers," J. Appl. Phys., vol.71, pp.1109-1115 (1992).
4) K. Takehisa "New designs and simulations of a 10 kW-average-power longitudinally-pumped dye laser amplifier," Appl. Optics, to be published.
5) K. Takehisa, and A. Miki, "Method for pumping a Ti:sapphire laser with a stable resonator copper vapor laser," Appl. Optics, vol.31, pp.2734-2737 (1992).